Strongly resonating bosons in hot nuclei

S. Zhang, A. Bonasera, M. Huang, H. Zheng, D. X. Wang, J. C. Wang, L. Lu, G. Zhang, Z. Kohley, Y. G. Ma, and S. J. Yennello

Phys. Rev. C **99**, 044605 — Published 16 April 2019

DOI: 10.1103/PhysRevC.99.044605

Strongly Resonating Bosons in Hot Nuclei

S. Zhang,[1,*] A. Bonasera,[2,3] M. Huang,[1,†] H. Zheng,[4] D.X. Wang,[1] J.C. Wang,[1] L. Lu,[1] G. Zhang,[5,6] Z. Kohley,[2,7] Y.G. Ma,[5,6,8] and S.J. Yennello[2,7]

[1]*College of Physics and Electronics information, Inner Mongolia University for Nationalities, Tongliao, 028000, China*
[2]*Cyclotron Institute, Texas A&M University, College Station, TX 77843, USA*
[3]*Laboratori Nazionali del Sud, INFN, via Santa Sofia, 62, 95123 Catania, Italy*
[4]*School of Physics and Information Technology, Shaanxi Normal University, Xian 710119, China.*
[5]*Key Laboratory of Nuclear Physics and Ion-beam Application (MOE), Institute of Modern Physics, Fudan University, Shanghai, 200433, China.*
[6]*Shanghai Institute Applied Physics, Chinese Academy of Sciences, Shanghai, 201800, China.*
[7]*Chemistry Department, Texas A&M University, College Station, Texas 77843, USA*
[8]*University of the Chinese Academy of Sciences, Beijing, 100080, China.*

When two heavy ions near the Fermi energy collide, a warm and low-density region can form in which fragments appear. This region is mainly dominated by proton (p) and alpha (α) particles. In such an environment, the αs interact with each other, and especially through strong resonances, form complex systems such as ^{8}Be and ^{12}C. Our experiments show that in the reactions $^{70(64)}$Zn(^{64}Ni)+$^{70(64)}$Zn(^{64}Ni) at E/A=35 MeV/nucleon levels of ^{8}Be appear around relative energies E_{ij}=0.092 MeV, 3.03 MeV as well as above 10 MeV and 100 MeV. We propose a different method to derive the correlation function based on the relative transverse energy distribution to minimize the experimental uncertainties. For the 3α systems, multi resonance processes give rise to excited levels of ^{12}C. In particular, the Hoyle state at 7.654 MeV excitation energy shows a decay component through the ground state of ^{8}Be and also components where two different α couples are at relative energies consistent with the ground state of ^{8}Be at the same time.

PACS numbers: 25.70.Pq
Keywords:

I. INTRODUCTION

Several decades after the suggestion given by Fred Hoyle [1] of a 0^+ resonance near the 3α threshold to accelerate ^{12}C formation in stars, the Hoyle state (HS) is still a hot topic in nuclear structure [2–16]. While its energy, i.e., 7.654 MeV, and width, 8.5 eV, are firmly established, there are debates on its decay. It is commonly accepted [5–16] that almost 100% of the HS decay is through the ground state of ^{8}Be (^{8}Be$_{g.s.}$), thus corresponding to a sequential decay (SD), i.e., first an α particle is emitted, and then ^{8}Be decays into 2αs with 0.092 MeV relative kinetic energy. Other decay modes, for example, the theoretically predicted direct decay (DD) of ^{12}C into 3αs of equal energy (DDE) or into a linear chain (LD) [4, 5] have been studied in high precision/high statistics experiments [8–16] giving an upper limit of 0.043%[14], 0.036%[15] and 0.024%[15] for DD, DDE, and LD, respectively. While we are probably at the limit of the experimental sensitivity, higher statistics experiments might be performed, or different strategies might be explored. In this paper, we will discuss a completely new approach, i.e., we will generally explore the ^{12}C decays also in the presence of nearby nuclear matter. This is surely relevant since stellar processes, where ^{12}C (or larger nuclei) are formed, might occur inside a dense star or on its surface, thus occurring under different conditions of density and temperature. One way to simulate some stellar conditions is to collide two heavy ions at beam energies near the Fermi energy. In central/peripheral collisions of the two ions, first we have a gentle increase in the density which is slightly above the ground state density, ρ_0=0.16fm^{-3} [17, 18] as revealed by microscopic calculations and experiments [19–22]. The system expands while cooling, and for densities below (1/3-1/6)ρ_0, clusters start to appear; this is referred to as the freeze-out region. Not only are protons and alpha particles formed, but also nuclei of larger masses with neutron (N) and proton (Z) contents. Under such conditions, excited fragments might decay, and nearby small fragments might coalesce and form new nuclei. The study of the formation and decay of complex fragments in nuclear matter is of interest, and in particular, in this work, we will study the decay modes of ^{12}C and ^{8}Be in 3 and 2αs, respectively. To increase the statistics, we combined the results of 3 different experiments: ^{70}Zn+^{70}Zn, ^{64}Zn+^{64}Zn, and ^{64}Ni+^{64}Ni all at 35 MeV/nucleon [23] and checked that each system separately produced results in agreement with the others at least for the observables discussed in this paper. There are many reasons for studying decays in nuclear fragmentation, in particular:

1) In nuclear matter, the levels and widths of decaying nuclei might be shifted/modified because of the interaction

with nearby species. For example, a change in the width of a resonance as compared to the vacuum might tell us the time duration of the freeze-out region.

2) Levels not observed in a vacuum might appear in the surrounding medium, for example, if many αs are formed at relative kinetic energies where E_{ij}=0.092 MeV, which is the binding energy of the $^{8}Be_{g.s.}$, then strong resonances among these bosons could give rise to correlations and Bose Einstein Condensation (BEC) [20, 24]. These conditions might be identified with the strong resonance region in microscopic calculations of the structure of ^{12}C [5, 21]. If this is a new state of ^{12}C as yet unobserved, it could be assigned as an Efimov state (ES). This is a general feature first predicted for nuclear systems [24, 25] and only observed in atomic systems [26, 27].
3) Are the decay modes of a particular resonance modified in medium? For example, is the SD of the HS still dominant with respect to the DD?
4) The SD dominance of the HS tells us that the relative kinetic energy of two αs is 0.092 MeV. What is the relative kinetic energy of the third α with respect to the first two? Why is the HS located at 7.654 MeV?

These and many other questions prompted us to follow an unconventional approach to nuclear structure and decay. The important tool is the detector, which must measure the energy and angle of fragments ejected from heavy-ion collisions to a high precision.

The paper is organized as follows: Section II summarizes the method of selecting and reconstructing events to analyze the important ingredients from relative kinetic energy distributions of 2αs. In section III, we discuss further particular decay modes of ^{12}C. We finally conclude and summarize our work in Section IV.

II. METHOD AND RESULTS

We analyzed the data from the experiments performed at the Cyclotron Institute, Texas A&M University [22, 23], using the NIMROD 4π detector [28]. Experimental details can be found in the Refs. [21–23, 28]. Here, it suffices to discuss the approach we follow in this paper. The detector measures the charge Z and mass A of each fragment up to Z=30 and A=50 on an event-by-event basis [23, 29]. From all the collected events, we selected 3α events, and the analysis was performed only on them. The momenta of the αs are rather well measured with the only major problem arising when the relative kinetic energy of the 2αs is small, of the order of tens keV. Such particles are detected in two nearby detectors (or in the same one) of NIMROD, and because of the detector's finite granularity, an error results in the angle and consequently for the relative momenta. This is a problem for all detector types and the resulting error or minimum relative kinetic energy which can be measured is of the order of 40 keV [8, 9]; the larger the granularity, the smaller the error. An evident advantage of our method, since we are working at the beam energy close to the Fermi energy, is that each ion has high kinetic energy, larger than few MeV/nucleon [23, 29]. This is optimal for our detector. It is the relative kinetic energy between α particles that needs to be small in order to reveal low energy excited levels of ^{8}Be and ^{12}C.

We emphasize that only the events with α multiplicity equal to three are analyzed in our analysis. Let us start by recalling the relation that calculate the excitation energy E^* of ^{12}C decaying into 3αs with Q-value, Q=-7.275 MeV. This relationship is given by Eq. (1):

$$E^* = \frac{2}{3}\sum_{i=1,j>i}^{3} E_{ij} - Q, \tag{1}$$

where E_{ij} is the relative kinetic energy of 2α and is measured event-by-event. Thus, we can easily estimate Eq.(1). Notice that the important ingredients entering Eq.(1) are the relative kinetic energies; since we have three indistinguishable bosons, we analyze the E_{ij} distribution by cataloging for each event the smallest relative kinetic energy, E_{ij}^{Min}, the middle relative kinetic energy, E_{ij}^{Mid}, and the largest relative kinetic energy, E_{ij}^{Lar}.

In Fig. 1, we plot the relative kinetic energy distributions for these three cases. In the top panels, the solid black circles give the distributions obtained from the real events. They show bumps but no real structures. This is due to the fact that in the fragmentation region, some α may come from the decay of ^{8}Be or ^{12}C or they might come from completely non-correlated processes, for example, the α emission from a heavy fragment [23, 29]. To distinguish the correlated from the non-correlated events, we randomly choose three different α from three different events and build the distributions displayed in Fig. 1 (mixing events-red open circles). The total number of real and mixing events are normalized to one, respectively. The two distributions look similar in log-scale but show some remarkable differences at low relative kinetic energies. While the distribution of the real events in Fig. 1(a) goes down, it goes up in Fig. 1(b) and (c) when the relative energy is not large. As we have mentioned, when the relative kinetic energy becomes very small, it becomes difficult to assign the angle of detection because of the detector granularity. This is, of course, less important for the Fig. 1(b) and (c) cases since the smallest relative kinetic energies are obtained for the events in

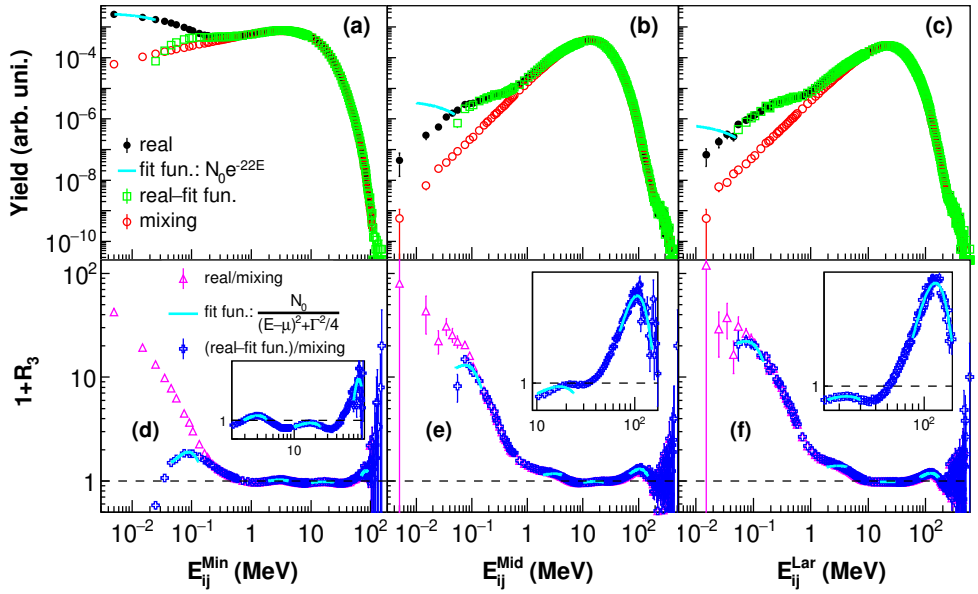

FIG. 1: (color online) Selected events from $^{70(64)}$Zn(^{64}Ni) + $^{70(64)}$Zn(^{64}Ni) at E/A=35 MeV/nucleon with α multiplicity equal to three. Relative kinetic energy distribution as a function of (a) the minimum relative kinetic energy, (b) the middle relative kinetic energy and (c) the largest relative kinetic energy of 2αs. The solid black circles represent data from real events, red open circles are from mixing events, and the green open squares represent the difference between the real events and the exponential function (solid line), which takes into account the experimental error. The ratios of the real (pink open triangles) data and the real data minus the fitting function (blue crosses) divided by the mixing events are, respectively, a function of (d) the minimum relative kinetic energy, (e) the middle relative kinetic energy and (f) the largest relative kinetic energy of 2αs. The solid lines are Breit-Wigner fits.

the first panel. To correct this feature, we fit the highest points of Fig. 1(a) with an exponential function. This allows us to derive the instrumental error ΔE=1/22 MeV=0.045 MeV, see Fig. 1(a). The estimated error is slightly larger than what is found in the Refs. [8–16] but small enough to let us derive the results discussed below. For Fig. 1(b) and (c), it is evident that the experimental error is less important and a change in slope can be seen around 0.1 MeV (the ^{8}Be$_{g.s.}$). To uncover the resonance, we can perform an exponential fit using the same slope (or experimental error) as before and fit the experimental point at 0.045 MeV. By subtracting the fits from the real events, we obtain the open squares in Fig. 1, which can be considered as the real events corrected by the detector acceptance. As we can see, all three cases display a bump around 0.08 MeV (very close to 0.092 MeV) corresponding to the decay of ^{8}Be$_{g.s.}$. Because of the way we have ordered the 2α's relative kinetic energies, we can deduce that if the largest relative kinetic energy is 0.092 MeV, the other two must be 0.092 MeV as well (since they are smaller). Thus, we have events where the 3αs are in mutual resonance, which is a mechanism similar to the Efimov states where a Boson is exchanged between the other two [24, 25, 30]. If this cannot be associated with a feature of a strongly resonating Boson gas [5], it might be an unexplored state of ^{12}C at E*=7.458 MeV (as given by Eq.(1)). In Ref. [31], the possibility of such a state was discussed, and it was suggested that its observation probability is 8-orders of magnitude smaller than the HS. Of course those calculations were in a vacuum; when in a medium, the mechanism of mutual resonances might be enhanced in the presence of other fragments, which could be more complex Bosons (for example, ^{16}O) or Fermions (for example, ^{7}Li). Taking the ratio of the real (minus the exponential fit) and the mixing events gives the correlation functions 1+R$_3$ displayed in the bottom panels of Fig. 1. The ratio shows that not only are peaks present around 0.08 MeV for all cases, but also at 3.05 MeV corresponding to the 1st excited level of ^{8}Be for the smallest relative kinetic energies, and higher energy peaks are also visible.

TABLE I: The parameters of BW fit to peaks in Fig. 1

	E_{ij}^{Min}: μ(MeV)	$\hbar/\Gamma$(fm/c)	E_{ij}^{Mid}: μ(MeV)	$\hbar/\Gamma$(fm/c)	E_{ij}^{Lar}: μ(MeV)	$\hbar/\Gamma$(fm/c)
peak1	0.088±0.001	1192±66	0.08±0.02	1089±288	0.08±0.04	984±540
peak2	3.05±0.01	14.2±0.3				
peak3	17.0±0.1	2.08±0.04			22.9±0.3	1.1±0.1
peak4	83±3	2.8±1.0	106±1	0.95±0.04	124.1±0.9	0.70±0.02

A Breit-Wigner (BW) fit to these resonances gives the parameters reported in Table I. No clear peaks can be seen for the 3.05 MeV and 17.0 MeV cases in Fig. 1(e) and (f). We used the same fitting values obtained in Fig. 1(d) for the 3.05 MeV and 17.0 MeV cases in Fig. 1(e) and for the 3.05 MeV case in Fig. 1(f). For the largest relative kinetic energy case, Fig. 1 (f), a peak appears around 23 MeV. As we can see, the centroids of the resonances are in good

agreement with values in a vacuum, but the widths are somehow larger either due to the experimental acceptance or, most probably, to the presence of a medium. These differences from the vacuum values are more marked for higher energies in the region 10-20 MeV where we know there are many resonances in ^{8}Be. Some of these resonances have large widths and others have narrow widths [32]. Probably, when in a medium, the effects in the freeze-out region are responsible for this feature, and if the width is associated with the lifetime of the system, then we can derive the value $\tau = \hbar/\Gamma \cong 1$ fm/c. There are no reported levels of ^{8}Be (or ^{12}C) around 100 MeV; thus, we could associate these bumps with some or many unobserved new levels at high excitation energies. However, it should be noted that the corresponding excitation energy per particle of ^{12}C: E*=100/12 MeV =8.33 MeV is very close to the center of mass energy in the heavy-ion collisions E$_{cm}$=35/4 MeV=8.75 MeV. Thus the correlation at such high energies might be due to the formation of a hot Boson-Fermion gas mixture and has been analyzed in some detail in Refs. [20–22]. A detector efficiency problem cannot be excluded since high energy αs move in the forward direction into the beam hole and thus remain undetected. The latter might be the correct explanation and it is supported by the fact that the centroid energy changes for different relative energies, last row in Table I. The lifetime of such a system is of the order of 1 fm/c. It is interesting to notice that the quantity 1+R$_3$ is smaller than one in the energy region above 10 MeV and becomes larger than one around 100 MeV (recall that the real and mixing events are normalized to the same area).

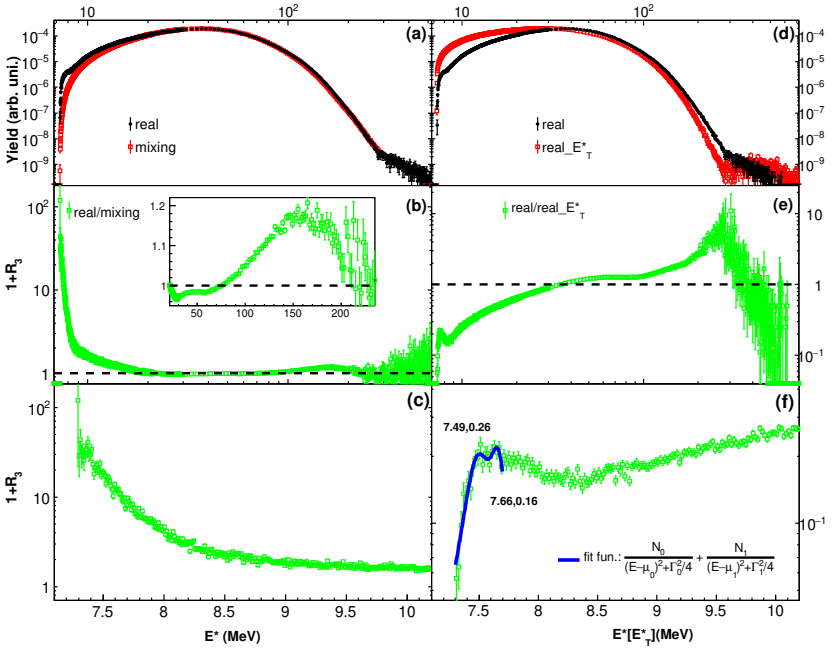

FIG. 2: (color online) The excitation energy distributions of the ^{12}C from 3αs. The solid black circles are the real events, red open squares are mixing events (or real transverse events), green open squares indicate the ratios of the real and mixing events (or real transverse events), and blue solid line is the BW fit.

III. DECAY MODES OF ^{12}C

In this work, the excitation energy E* of ^{12}C from 3αs are also reconstructed using Eq.(1). The excitation energy distributions of the real events (solid black circles) and the mixing events (red open squares) are plotted in Fig. 2(a), and their ratio (1+R$_3$) (green open squares) in Fig. 2(b, c) with different energy windows. We can see that there is a sharp peak below E*=8 MeV. This feature is an effect of the finite granularity of the detectors that, especially at low relative excitation energies, are not able to reveal fine structures. We notice that at high relative energies the 1+R$_3$ is approximately equal to one which indicates that the available phase space is dominated by statistical processes. This feature suggested us a different procedure to minimize the effects of the detector low granularity. In fact if the system reaches thermal equilibrium, one can look at the α transverse relative kinetic energy distribution. The advantage of this procedure is that instead of producing mixing events to derive the available phase space, we can derive the transverse kinetic energy distribution from the same real events. When the ratio of the real events and the real transverse events is derived, the detector error might cancel out or becomes less important. This is a new method to study correlation functions. Similar to Eq.(1) we define the transverse excitation energy as:

$$E_T^* = \frac{2}{3}\sum_{i=1,j>i}^{3}\frac{3}{2}(E_{ij}^X + E_{ij}^Y) - Q, \tag{2}$$

where E_{ij}^X and E_{ij}^Y are the relative kinetic energy of 2α in X and Y directions (Z is the beam axis direction).

In Fig. 2(d,e,f), the transverse excitation energy of the real events (red open squares) are also included. We can see that there is a clear broad peak around 7.6 MeV in Fig. 2(f). From the BW fit to this broad peak, the parameters of the centroids at 7.49 MeV (ES of ^{12}C) and at 7.66 MeV (HS of ^{12}C) are obtained.

In order to increase our confidence in the new proposed method, we reconstruct the excitation energy E* of ^{3}Li from 3 proton events. We arbitrarily assign Q=-7.275 MeV which is the Q-value of ^{12}C for easy comparison to the 3α case. No peaks are observed when the transverse energy distribution is used, while the mixing technique shows a huge bump at low relative energies similar to the ^{12}C case leading to the conclusion that it is the detector finite acceptance which produces the 'bump'.

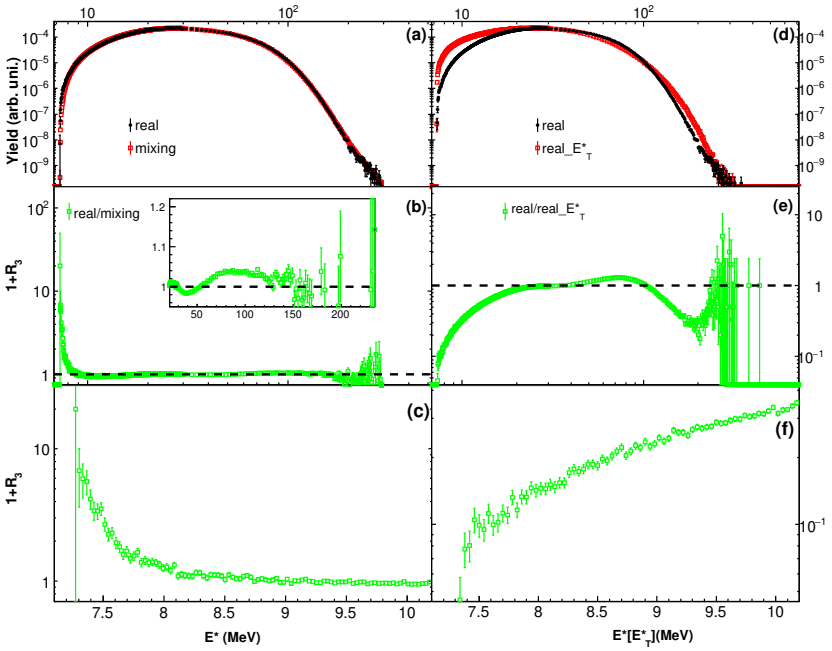

FIG. 3: (color online) The excitation energy distributions of the ^{3}Li from 3 proton events, where we have arbitrarily assigned Q=-7.275 MeV for easy comparison to Fig. 2. The solid black circles are the real events, red open squares are mixing events (or real transverse events), green open squares indicate the ratios of the real and mixing events (left panels) or real transverse events (right panels).

In order to strengthen the above results, we derived observables which give the probability of ^{12}C decay into a particular mode (say the 3αs relative kinetic energies are equal (DDE) or two energies are equal and the third one is twice the sum of the first two (LD)) with respect to SD. These probabilities have been discussed experimentally using different techniques [8–16]; thus, it is especially interesting to compare our results in a medium with conventional approaches. Notice that the effects in a medium might be present in Ref. [9] and this might explain the discrepancies from conventional approaches [8–16]. We define the decay probability as Eq.(3):

$$\prod(E^*, \delta E) = \frac{\sum_{ij}[Y_R(DDE\,or\,LD, E_{ij}) - Y_M(DDE\,or\,LD, E_{ij})]}{\sum_{ij}[Y_R(SD, E_{ij}) - Y_M(SD, E_{ij})]}, \tag{3}$$

where the sum is extended over all relative kinetic energies corresponding to a ^{12}C level with excitation energy E* from Eq.(1) and variance δE, which we will vary to the smallest values allowed by the statistics. The Y_R(SD, E_{ij}) and Y_M(SD, E_{ij}) in the denominator are obtained by fixing the smallest relative kinetic energy to the ^{8}Be$_{g.s.}$ $\pm$ δE/3 for the real (R) and mixing (M) events, respectively. The yields of DDE or LD are obtained by opportunely choosing the relative kinetic energies in the numerator. For example, the DDE case is obtained by choosing three equal relative kinetic energies (within δE/3 for each one). For a fixed excitation energy, we can estimate Eq.(3) from the data by changing δE in order to derive the limiting value of the ratio compatible with the experimental sensitivity.

In Fig. 4, we plot the ratios for the DDE (top panel) and the LD (bottom panel) as a function of δE (normalized to the kinetic contribution to E* from Eq.(1)). The ES (E*=7.458 MeV) and the HS (E*=7.654 MeV) cases are given, respectively, by the solid (black) circles and the solid (red) squares. We have divided the ES cases by the HS SD, thus

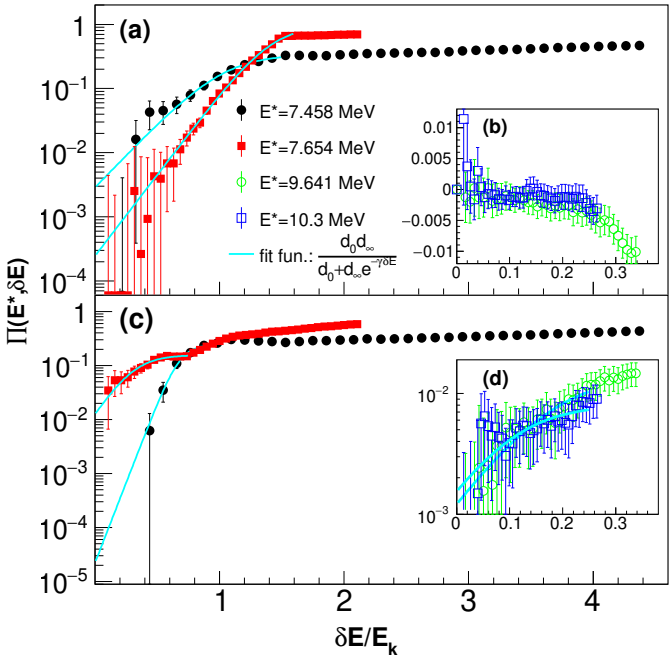

FIG. 4: (color online) The probability ratios of the DDE (top) and LD (bottom) as a function of the error (normalized to the kinetic contribution to E* from Eq.(1)).

these ratios give the decay probabilities of the ES with respect to the HS. The 9.641 MeV (green open circles) and the 10.3 MeV (blue open squares) are given in the insets. The ratios can be reproduced by the function [33] given by Eq.(4):

$$\prod(E^*, \delta E) = \frac{d_0 d_\infty}{d_0 + d_\infty e^{-\gamma \delta E}}. \tag{4}$$

The parameter d_0 (δE$\rightarrow$0) gives the smallest possible physical value of the ratios or the experimental error, while the largest value d_∞ (δE$\rightarrow\infty$) is connected to the available phase space [33]. The fit values of d_0 are reported in Table II and are compared to the data in literature. Since Ref. [9] might contain effects from within a medium as in our case, we argue that the difference is due to not properly subtracting the mixing events when calculating the ratios, as in Eq.(3). Another possibility is the contribution of the ES due to the experimental sensitivity. We can see that the LD contribution of the ES is compatible with zero, which is consistent with the definition of the ES. For the larger excitation energies considered here, the ratios are negative for the DDE case (see Fig. 4(b)) and compatible with zero for the LD case (see Fig. 4(d)).

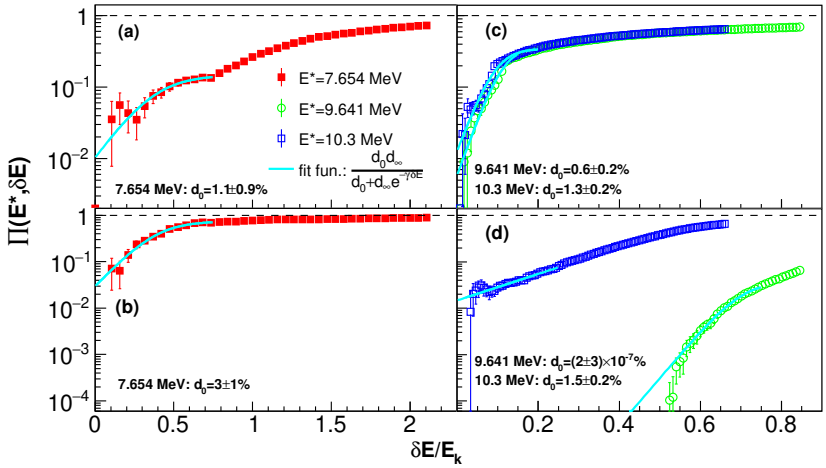

FIG. 5: (color online) The probability ratios of the HS (a) when the ^{8}Be$_{g.s.}$ energy is consistent with two α relative kinetic energies, or (b) the second largest energy is twice of the ^{8}Be$_{g.s.}$ energy. The ratios are plotted for 9.641 MeV (green open circles) and 10.3 MeV (blue open squares), (c) when the E_{ij}^{Min}=0.092 MeV, E_{ij}^{Mid}=E_{ij}^{Lar}, or (d) the E_{ij}^{Lar}=3.03 MeV, E_{ij}^{Min}+E_{ij}^{Mid}=$\frac{3}{2}$×(E* + Q) - E_{ij}^{Lar}.

TABLE II: Fit values of the parameter d_0 compared to Refs. [5, 9–13, 15, 31]

	ES:DDE(%)	ES:LD(%)	HS:DDE(%)	HS:LD(%)	9.641:DDE(%)	9.641:LD(%)	10.3:DDE(%)	10.3:LD(%)
Present	0.3±0.1	0.002±0.004	0.025±0.005	1±1	0	0.1±0.1	0	0.2±0.2
Ref.[9]			7.5±4.0	9.5±4.0	0			
Ref.[12]			0.3±0.1	0.1				
Ref.[10]			0.45					
Ref.[15]			0.036	0.024				
Ref.[11]			0.09	0.09				
Ref.[13]			0.08					
Ref.[5]			0.005	0.03				
Ref.[31]			0.0036					

Not only the excited levels of ^{8}Be determine the SD modes of ^{12}C but also multiple integers of the ^{8}Be$_{g.s.}$ energy. In the left panels of Fig. 5, we have plotted the ratios for the HS when the ^{8}Be$_{g.s.}$ energy is consistent with E_{ij}^{Min} and E_{ij}^{Mid} (Fig. 5(a)) or the E_{ij}^{Mid} is twice of the ^{8}Be$_{g.s.}$ (Fig. 5(b)). In the right panels of Fig. 5, the ratios are plotted for 9.641 MeV and 10.3 MeV, when the E_{ij}^{Min}=0.092 MeV, E_{ij}^{Mid}=E_{ij}^{Lar} (Fig. 5(c)), or the E_{ij}^{Lar}=3.03 MeV, E_{ij}^{Min}+E_{ij}^{Mid}=$\frac{3}{2}$×(E* + Q) - E_{ij}^{Lar} (Fig. 5(d)). There are decay modes with those conditions, in particular, when the relative kinetic energies are approximately equal to the ratio 1:2:3, a (3±1)% contribution to SD results for the HS, see Fig. 5(b).

IV. SUMMARY AND CONCLUSION

In this work, we have discussed energy levels of ^{8}Be and ^{12}C in hot nuclear matter. We found that the DDE and LD decay modes are strongly depleted. Thus the decay probability is mainly determined by the ^{8}Be formation probability in ^{12}C. Depending on the excitation energy of ^{12}C, ^{8}Be might be formed, not only in the ground state, but also in excited states as well. We confirm the finding of Ref. [34] that some decay modes are dominated by ^{8}Be levels hit more than once. A special case is the ES when the relative energies of 3αs are consistent with the ^{8}Be$_{g.s.}$, a signature of a strongly resonating Boson gas or an Efimov state, consistent with observations in atomic systems Ref. [26]. Some DDE and LD decay modes might be observed at very large excitation energies and these will be discussed further in a following work together with the question of BEC. We have discussed a new method to obtain the correlation function by using the transverse relative kinetic energy instead of the mixing events technique. This reduces the uncertainty due to the detector finite granularity, but ambiguities still remain especially on the question if there might be a resonance in ^{12}C below the Hoyle state [31, 35]. This 'resonance' might be due to the 3αs going through the ^{8}Be$_{g.s.}$ resonance at the same time, a mechanism introduced for Efimov states [24–27, 35]. It might be an effect which occurs in hot nuclear matter only and not necessarily a new excited level in ^{12}C which could be tested in higher statistics experiments without in medium effects. A dedicated experiment with higher statistics and better detector system, say for ^{40}Ca+^{40}Ca collisions around 40 MeV/nucleon, should shed further light on the properties of the resonating bosons in hot matter.

ACKNOWLEDGMENTS

This work was supported by the National Natural Science Foundation of China (No. 1176014, 11605097, 11421505, 11865010), the US Department of Energy under Grant No. DE-FG02-93ER40773, NNSA DE-NA0003841 (CENTAUR) and the Robert A. Welch Foundation under Grant No. A-1266. This work was also supported by the Chinese Academy of Sciences (CAS) President's International Fellowship Initiative (No. 2015VWA070), Strategic Priority Research Program of the Chinese Academy of Sciences (No. XDB16 and XDPB09), Program for Young Talents of Science and Technology in Universities of Inner Mongolia Autonomous Region (NJYT-18-B21) and Doctoral Scientific Research Foundation of Inner Mongolia University for Nationalities (No. BS365 and BS400), The Fundamental Research Funds for the Central Universities (No. GK201903022), Natural Science Foundation of Inner Mongolia(No. 2018MS01009). AB thanks the Chinese Academy of Science, Sinap and Inner Mongolia University of Nationalities for the warm hospitality and support during his stay in China while this work was completed.

* E-mail at:zsylt@imun.edu.cn
† E-mail at:huangmeirong@imun.edu.cn

[1] F. Hoyle, Astrophys. J. Suppl. Ser. **1**, 121 (1954).
[2] D. J. Marín-Lámbarri *et al.*, Phys. Rev. Lett. **113**, 012502 (2014).
[3] E. Epelbaum *et al.*, Phys. Rev. Lett. **106**, 192501 (2011).
[4] Y. Kanada-En'yo, Prog. Theor. Phys. **117**, 655 (2007).
[5] S. Ishikawa, Phys. Rev. C **90**, 061604 (2014).
[6] H. Morinaga, Phys. Lett. **21**, 78 (1966).
[7] M. Freer and H. O. U. Fynbo, Prog. Part. Nucl. Phys. **78**, 1 (2014).
[8] M. Freer *et al.*, Phys. Rev. C **49**, R1751 (1994).
[9] Ad. R. Raduta *et al.*, Phys. Lett. B **705**, 65 (2011).
[10] J. Manfredi *et al.*, Phys. Rev. C **85**, 037603 (2012).
[11] O. S. Kirsebom *et al.*, Phys. Rev. Lett. **108**, 202501 (2012).
[12] T. K. Rana *et al.*, Phys. Rev. C **88**, 021601 (2013).
[13] M. Itoh *et al.*, Phys. Rev. Lett. **113**, 102501 (2014).
[14] D. Dell'Aquila *et al.*, Phys. Rev. Lett. **119**, 132501 (2017).
[15] R. Smith *et al.*, Phys. Rev. Lett. **119**, 132502 (2017).
[16] O. Kirsebom, Physics **10**, 103 (2017).
[17] G. Giuliani, H. Zheng, A. Bonasera, Progress in Particle and Nuclear Physics **76**, 116 (2014).
[18] A. Bonasera, F.Gulminelli, J.Molitoris, Physics Reports **243**, 1 (1994).
[19] H. Suno, Y. Suzuki and P. Descouvemont, Phys. Rev. C **94**, 054607 (2016).
[20] P. Marini *et al.* [INDRA Collaboration], Phys. Lett. B **756**, 194 (2016).
[21] K. Schmidt *et al.*, Phys. Rev. C **95**, 054618 (2017).
[22] J. Mabiala, H. Zheng, A. Bonasera, Z. Kohley and S. J. Yennello, Phys. Rev. C **94**, 064617 (2016).
[23] Z. Kholey, 2010 PhD Thesis, Texas A &M University.
[24] V. Efimov, Phys. Lett. B **33**, 563 (1970).
[25] V. Efimov, Nat. Phys. **5**, 533 (2009).
[26] M. Zaccanti, et al., Nat. Phys. **5**, 586 (2009).
[27] C.H. Greene, Phys. Today **63 (3)**, 40 (2010).
[28] https://cyclotron.tamu.edu/nimrod
[29] S. Zhang, J.C. Wang, A. Bonasera, *et al.*, Chinese Physics C, Submitted (2019).
[30] P. Naidon and S. Endo, Rept. Prog. Phys. **80**, 056001 (2017).
[31] H. Zheng, A. Bonasera, M. Huang, S. Zhang, Phys. Lett. B **779**, 460 (2018).
[32] http://www.nndc.bnl.gov
[33] H.G. Schuster, Deterministic Chaos, Weinheim; New York, VCH, 1995.
[34] A. Tumino *et al.*, Phys. Lett. B **750**, 59 (2015).
[35] H. Zheng and A. Bonasera, arXiv:1811.10412.